# Assessing Performance of an Extremum Seeking Controller Using Continuation Methods

Duc H. Nguyen, Mark H. Lowenberg, and Simon A. Neild

***Abstract* — In order to assess the performance of an extremum seeking controllers, many restrictive assumptions have to be made due to the presence of a harmonic forcing signal, and the process remains mathematically intensive. We propose the use of bifurcation analysis and numerical continuation to provide a simple numerical framework to investigate the dynamics of an extremum seeking system. Using the example of a poorly-tuned auto-trim system on a nonlinear airliner model, the advantage of bifurcation analysis and continuation is demonstrated, including the ability to directly identify the oscillation amplitude and stability information. Other behaviours common in nonlinear harmonically-forced systems, such as existence of multiple solutions and bifurcations leading to multi-harmonic responses, are also detected. The purpose of this paper is to demonstrate the advantages of continuation in characterising the dynamics of an extremum seeking controller and to present this promising controller scheme to the wider aeronautics audience.**

## I. Introduction

Extremum seeking control is a form of model-free adaptive control that automatically seeks out the extremum point(s) (maxima or minima) of an objective function. This is done via a 'perturb and observe' scheme, which injects a sinusoidal perturbation to the control signal and observes the subsequent changes in the objective function. An online estimation of the objective function's slope can then be inferred, which in turn drives the control input to the point at which the slope is zero (i.e., the extremum). As the whole process is done online and does not require any knowledge of the plant, extremum seeking control is especially useful in cases where the optimal set point is either not known or is highly sensitive to changes in parameters, as often seen in many real-world applications.

Extremum seeking control has attracted significant attention from researchers in recent years. Specifically, the number of publications on the topic between 2000 and 2009 alone exceeded those from the year 1960 to 2000 combined [1]. Part of the reason for this sudden surge in interest is due to a pivotal paper in 2000, which provided the first rigorous mathematical proof of stability in a general nonlinear extremum-seeking system [2]. Since then, various engineering and industrial applications of extremum seeking control have been explored, including maximising pressure rise in an aero-engine compressor [3], optimising power output of wind turbines [4], and minimising power demand during formation flight [5], to name a few. On the theoretical front, some notable works include automatic tuning of PID gains [6], limit cycle amplitude minimisation [7], convergence analysis [8], and optimising systems with only periodic solutions [9]. Another recent development is the addition of a built-in extremum-seeking block in the Simulink Control Design toolbox of MATLAB R2021a [10]. This reflects the increasing popularity of the method and will further introduce extremum seeking control to many new users through a user-friendly environment. For a formal introduction to extremum seeking control and its applications, readers are referred to papers [1,11] and textbooks [12,13].

Despite these developments, the current procedures for analysing an extremum-seeking system remain mathematically challenging and involve a number of assumptions that may prove impractical in many engineering systems. This in large part is due to the presence of the harmonic perturbation, which results in periodic motions and poses a major challenge to both analytical and numerical analyses. Regarding the analytical side, the method of averaging and the singular perturbation method are employed to reduce the system under investigation and approximate it as an equilibrium map [2]. The assumptions involved in these approaches require that the frequencies of the three main elements (the perturbation signal, the filters in the extremum controller, and the plant's dynamics) are well separated [7] – usually by an order of magnitude each. Considering the example of a generic flight dynamics model, these requirements are already limiting since a simple longitudinal ($4^{th}$-order) aircraft model with actuator already spans three orders of magnitude on the frequency spectrum: $10^{-1}$-$10^{0}$ rad/s for the two rigid-body modes and $10^{1}$ rad/s for the actuator. The impact of higher-order harmonic terms is also neglected in these approximations, which may further invalidate the results in highly nonlinear applications. On the numerical front, recent works have successfully employed numerical continuation using the AUTO-07P software to analyse extremum seeking controllers [14-17]. Various nonlinear phenomena have been characterised using this continuation-based scheme, including existence of multiple stable solutions, unstable solutions, and loss of stability. However, the underlying equations used by the numerical solver in [14-17] are equilibrium approximations of the full harmonically-forced systems, so the limitations listed above still apply.

To fill in this gap, we present here an example of how harmonically-forced bifurcation analysis can be employed to analyse an extremum seeking controller on a highly nonlinear system with no closed-form solutions. This method effectively

All authors are with the Department of Aerospace Engineering, University of Bristol, Bristol, BS8 1TR UK.
Duc H. Nguyen (corresponding author, email: duc.nguyen@bristol.ac.uk)
Mark H. Lowenberg (email: m.lowenberg@bristol.ac.uk)
Simon A. Neild (email: simon.neild@bristol.ac.uk)

converts the harmonically-forced plant into an autonomous self-oscillating system, which can then be easily solved by continuation. Past applications of harmonically-forced bifurcation analysis have focused on examining the frequency response of nonlinear systems, most famously the Duffing equation (see section II in [18] for a brief introduction), along with some recent developments in the field of flight dynamics and control [18,19]. In presenting this work, we hope that the combination of bifurcation analysis and extremum seeking control will provide a powerful framework for future researchers and engineers to design and test many advanced implementations of this controller scheme. The example problem shown here can also be another contribution to the ever-expanding literature on dynamics of nonlinear harmonically-forced systems.

## II. Problem Description

In this paper, we consider a fourth-order longitudinal aircraft model coupled with a conventional manoeuvre-demand controller and an auto-trim system – the latter uses extremum seeking. Although both controllers provide stability and accomplish their objectives, they have been intentionally tuned to achieve poor performance. This provides the backdrop to demonstrate the capability of harmonically-forced bifurcation analysis to identify the stability boundaries and revealing the wide variety of dynamics that can be encountered in a poorly-designed controller or on a highly nonlinear plant.

### A. Aircraft Model and the Manoeuvre-Demand Controller

Using the notations in Table I, the open-loop equations of motion for the longitudinal rigid-body modes of an aircraft can be written

$$\dot{\alpha} = \frac{1}{mV}\left[\frac{1}{2}\rho V^2 S(C_z \cos\alpha - C_x \sin\alpha) - T\sin\alpha + mg\cos(\theta-\alpha)\right] + q \quad (1)$$

$$\dot{V} = \frac{1}{m}\left[\frac{1}{2}\rho V^2 S(C_z \sin\alpha + C_x \cos\alpha) + T\cos\alpha - mg\sin(\theta-\alpha)\right] \quad (2)$$

$$\dot{q} = \frac{1}{2}\rho V^2 Sc\frac{C_m}{I_y} - \frac{Th}{I_y} \quad (3)$$

$$\dot{\theta} = q \quad (4)$$

in which the coefficients of aerodynamic force along the body x and z axes $C_x$ and $C_z$ (forwards along the fuselage and downwards respectively) and the moment coefficient in pitch $C_m$ are represented as follows:

$$C_i = C_{i_0}(\alpha) + C_{i_1}(\alpha, \delta_e, \delta_t) + C_{i_2}(\alpha)\frac{cq}{2V} \quad (5)$$

where $i = [x, z, m]$. $\delta_e$ and $\delta_t$ are the two control inputs, representing the elevator and the all-moving tailplane deflections, respectively. Either input can be used to control the aircraft's attitude in the longitudinal plane. The force and moment coefficients in (5) are shown in Figure 1, depicting data from the NASA Generic T-tail Model (GTT) created to represent a generic mid-sized regional airliner. pchip and spline interpolation/extrapolation are used to make the model smooth, which is beneficial for bifurcation analysis. The remaining terms in (1-4) are constants listed in Table I.

TABLE I. Aircraft States and Parameters

| | | |
|---|---|---|
| $\alpha$ | angle of attack | STATES |
| $V$ | velocity | |
| $q$ | pitch rate | |
| $\theta$ | pitch angle | |
| $\delta_e$ | elevator deflection | INPUTS |
| $\delta_t$ | tailplane deflection | |
| $c$ | mean aerodynamic chord | 3.37 m |
| $g$ | gravitational acceleration | 9.81 m/s$^2$ |
| $h$ | thrust line distance above CG | 2.02 m |
| $I_y$ | pitch moment of inertia | 1,510,624 kg m$^2$ |
| $m$ | mass | 25,332 kg |
| $S$ | wing area | 70.1 m$^2$ |
| $T$ | thrust | 29,982 N |
| $\rho$ | air density (at 10,000 ft) | 0.905 kg/m$^3$ |

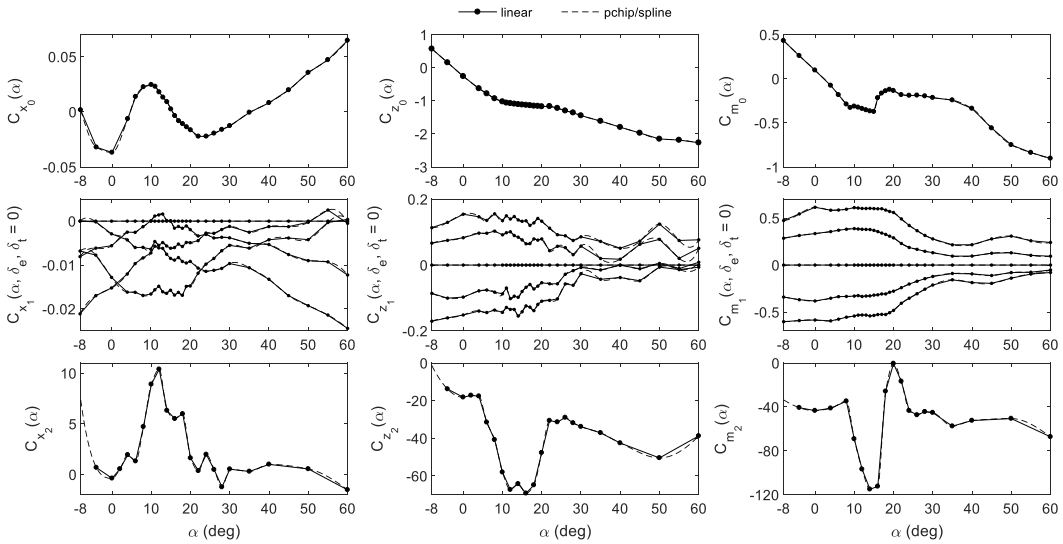


Figure 1. Aerodynamic coefficients of the GTT.

A simple angle-of-attack demand controller as shown in Figure 2a is used in our analysis. The reference input is demanded angle of attack $\alpha_d$, which is subtracted from the actual angle of attack in the outer loop and then integrated. In the inner loop, a proportional stability augmentation system is included using pitch rate $q$ and pitch angle $\theta$ feedback, providing pitch damping and stiffness, respectively. All three gains $K_I$, $K_q$, and $K_\theta$ are fixed gains. The block $C_E$ is the extremum-seeking controller used for auto-trim. Its input is the elevator deflection $\delta_e$ and the output is tailplane deflection $\delta_t$. The details of $C_E$ are presented in the next section. As mentioned, the closed-loop system is stable, although the gains have been selected to give poor performance.

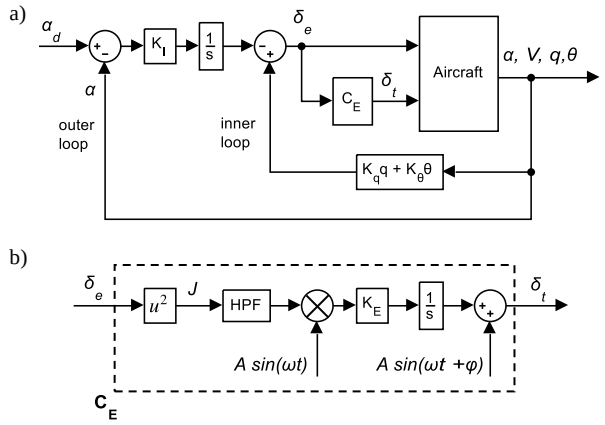


Figure 2. Closed-loop block diagrams.

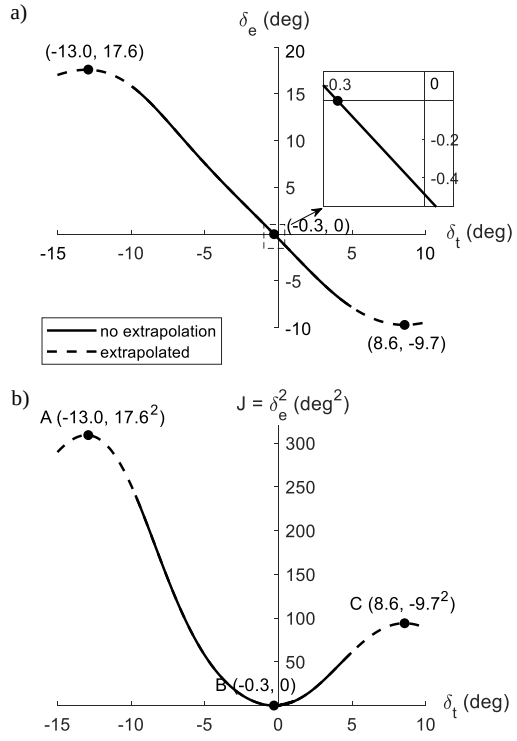


Figure 3. Static relationship between elevator and tailplane for trimmed flight at α = 2° (a) and the objective function (b).

## B. *The Extremum-Seeking Auto-Trim Controller*

An extremum-seeking controller will automatically seek out the maxima or minima of an objective function, which is usually the points with zero slope. In this example, the objective function is defined as $J = \delta_e^2$. The idea is that the controller will adjust the tailplane deflection until $\delta_e^2$ reaches its minimum at zero. When this condition is achieved, the aircraft will be flying at the commanded angle of attack using only tailplane for trim, which could represent minimum drag trim for the specific flight condition.

Since pitch control can be achieved using either elevator or tailplane deflection, there are multiple combinations of these control inputs that can be used to keep the aircraft flying at a constant angle of attack. The static relationship between elevator and tailplane deflections that maintains flight at $\alpha$ = 2 deg is shown as the solid line in Figure 3a, with the inset showing a magnified view. Only aerodynamic data for tailplane between –10 and +5 deg are available. However, they can be spline-extrapolated as shown by the dashed lines. This artificially creates a peak and a trough with zero slopes that can potentially draw the auto-trim controller toward them instead of the desired $\delta_e^2$ = 0 point. For our purpose, this artificial peak/trough pair is desirable as it allows us to demonstrate the full capability of continuation methods in identifying additional attractors that may be hard to detect. Therefore, spline extrapolation is used for the tailplane aerodynamic data. This results in the objective function $J = \delta_e^2$ as shown in Figure 3b, with the three zero-slope points labelled A-C; point B is the desired target for the auto-trim controller.

A brief introduction to the principles of extremum seeking control is now presented, although readers are referred to sources such as [12,13] for a more formal introduction. Figure 2b is the block diagram of the auto-trim controller. The input to the controller is elevator, which is automatically controlled by the $\alpha$-demand system. $J = \delta_e^2$ is the objective function as defined, which passes through a high pass filter to remove the bias. This signal is multiplied by a sinusoidal perturbation of the form $A\sin(\omega t)$ and a proportional gain $K_E$ and then integrated. Finally, another sinusoidal perturbation is added with a phase lag $\varphi$, giving us the tailplane deflection. In this scheme, the controller will continuously perturb the tailplane $\delta_s$ at a frequency $\omega$ rad/s, thereby causing $J$ to vary sinusoidally at the same frequency. The $\alpha$-demand controller will adjust $\delta_e$ in response to changes in $\delta_t$ by following the static map in Figure 3a to keep the angle-of-attack at 2 deg. The set point of $\delta_t$ is determined by the integral action, which continuously drives $\delta_t$ until $JK_EA\sin(\omega t)$ oscillates symmetrically about zero. This only happens when $J$ reaches one of the inflection points in Figure 3a (so that the product of $J(\omega t)$ and $\sin(\omega t)$ is symmetric about zero). The extremum seeking controller therefore has the capability to automatically seek out an inflection point in an objective function without any knowledge of the model – making it especially useful for plants that are sensitive to changes in system parameters. We acknowledge that a real-world auto-trim controller does not require extremum seeking [20-22] and the example provided here is only to exemplify the capability of bifurcation and continuation methods. For this study, the extremum controller

has the following parameters: $A$ = 0.1°, $K_E$ = 5, $\varphi$ = 0° with a high-pass filter cut-off frequency of $\omega_F$ = 6 rad/s.

The effects of both the $\alpha$-demand and the auto-trim controllers are now presented. Figure 4 shows the aircraft responding to a step change in demanded angle of attack from 1 to 2 deg using two different forcing frequencies – both are under 1 Hz and can therefore be considered realistic. In both instances, the angle of attack converges to its commanded value of 2 deg. However, the second case with 2.3 rad/s forcing fails to drive the elevator to zero, and instead converges to the inflection point C in Figure 3b. This does not happen when $\omega$ is increased to 5 rad/s, as seen in Figure 4a.

## III. Harmonically-Forced Bifurcation Analysis

Having discussed the basics of extremum control and its potential shortcomings in highly nonlinear applications, we now propose the use of bifurcation analysis and numerical continuation as a tool to systematically assess the performance in those situations. Since its first application to flight dynamics models in the early 80s [23,24], bifurcation analysis has seen increasing use in the field of aircraft dynamics and control by both the research community and the industry [25]. This method is typically used to trace out a map of equilibrium and limit cycle solutions – both stable and unstable – in a nonlinear system in response to static changes in an input parameter (such as control surface deflection). Past studies have successfully used bifurcation analysis to characterise various nonlinear behaviours of interest such as spin, wing rock, and jump phenomenon [26], as well as to assess the performance of flight control systems [27,28]. These studies, however, were still restricted to analysing quasi-static changes to the input parameter. A further extension the method in the flight dynamics context has been proposed recently, which permits examinations of the aircraft's responses to a harmonic forcing input; the results are then presented in the form of a nonlinear Bode plot [18,19]. The same approach is used here to analyse a closed-loop system with an extremum seeking controller, which is inherently periodic due to the presence of the sinusoidal perturbation. We refer to this approach as harmonically-forced bifurcation analysis in this paper.

The method to implement harmonically-forced bifurcation analysis in an extremum-seeking system is now presented. In general, bifurcation analysis requires that the state equations be written as autonomous first-order ordinary-differential equations. The harmonic forcing term $\sin \omega t$ (or other equivalent) can be generated in such an environment by the addition of two 'dummy states'

$$\dot{x}_1 = x_1 + \omega x_2 - x_1(x_1^2 + x_2^2) \quad (4)$$

$$\dot{x}_2 = -\omega x_1 + x_2 - x_2(x_1^2 + x_2^2) \quad (5)$$

It can be shown that $x_1 = \sin \omega t$ and $x_2 = \cos \omega t$ are asymptotically stable solutions of (4-5). These two states can now be used to generate the harmonic forcing signals in an extremum seeking controller (i.e., $A \sin \omega t$ becomes $Ax_1$). Accordingly, the whole plant is now a self-oscillating autonomous system, for which steady state solutions can be found by continuation in the same way as an autonomous (non-forced) system can be solved for limit cycle solutions.

All bifurcation analysis in this paper was done in the MATLAB/Simulink environment using the Dynamical Systems Toolbox [29], which is the MATLAB implementation of the continuation software AUTO-07P [30].

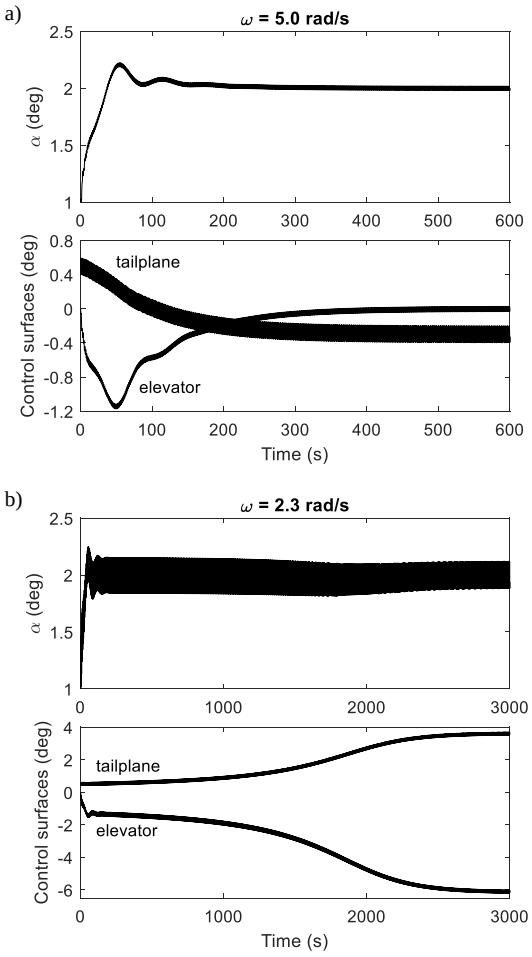


Figure 4. Responses to step change in $\alpha_d$ using two different forcing frequencies.

## IV. Results

The two different responses observed in Figure 4 suggest that there are at least two branches of stable solutions. Using these two responses as starting points for the continuation solver, the resulting bifurcation diagrams of the elevator and stabilator deflections are shown in Figure 5, in which panel a is the overal view and panels b and c are the magnified views. The forcing frequency $\omega$ is set as the continuation parameter, thereby giving us an indication of how our choice of $\omega$ affects the oscillation amplitude and stability. All solutions in Figure 5 are periodic, and both the maxima and the minima of the oscillation are shown (although the amplitudes are small so the maxima and minima are almost indistinguishable, apart from panel b). Therefore, the oscillation amplitudes are easily indentified on the diagram – a major advantage over existing methods that approximate the responses as equilibrium maps. The colours indidacate whether the solutions belong to the same family and can therefore be detected in one continuation run. In this instance, two separate branches are dectected,

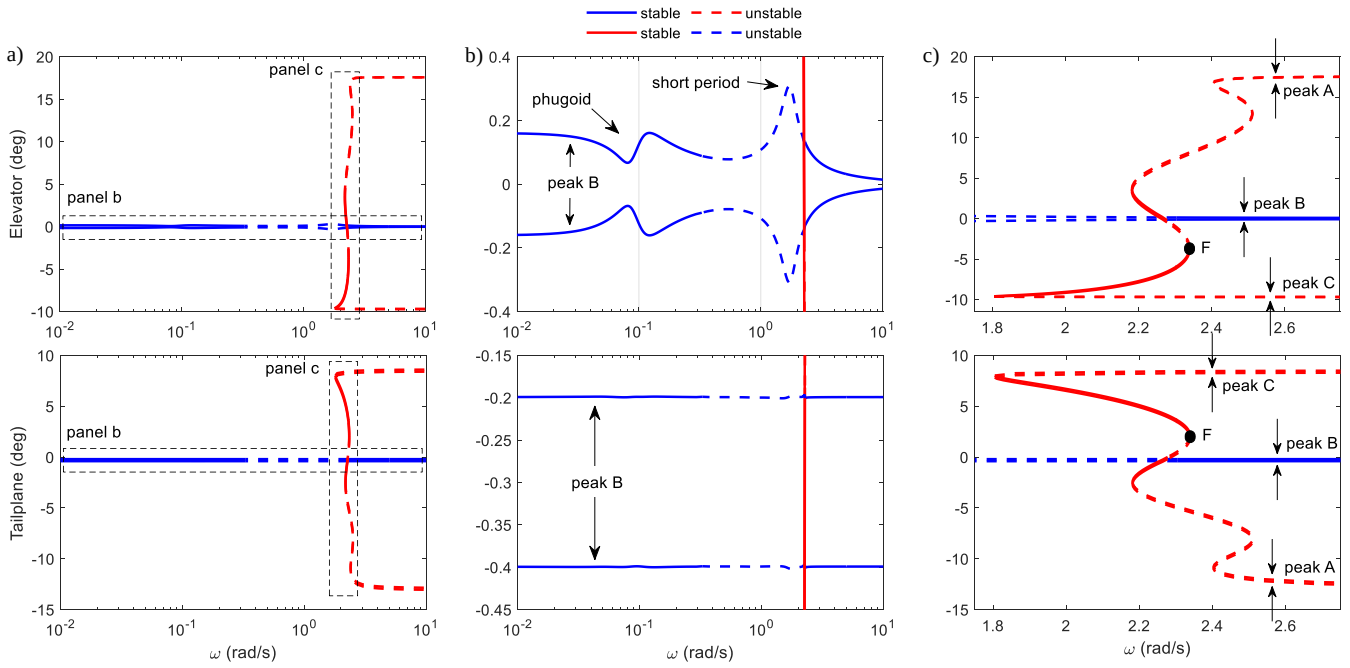


Figure 5. Bifurcation diagrams – $\omega$ continuation. Panels b and c are the magnified views.

which are henceforth referred to as the red and blue branchesPanels a and c indicate that when $\omega$ is sufficiently high (above 2.34 rad/s), there is only one stable solution from the blue branch corresponding to the $J = 0$ peak in Figure 3 – the desirable one. For $\omega$ between 0.33 and 2.34 rad/s, the response is either period-1 unstable, or converges to one of the stable solutions in the red branch. The high-frequency solutions corresponding to peaks A and C on the red branch are unstable due to the presence of the high-pass filter. Without it, these solutions become stable, resulting in a much more degraded controller. Numerical continuation is capable of detecting this change in stabilty, although this is not shown for brevity. It is also noted that the red and blue branches cross each other at a point that resembles a transcritical bifurcation (despite all solutions being periodic), although the crossing point is not detected by the continuation solver.

Point F in panel c is the boundary of $\omega$ that ensures the blue branch is the only stable solution during operation (unless $\omega$ is reduced to below 0.33 rad/s). This point is sensitive to the filter cutoff frequency $\omega_F$. To investigate this, we trace out the locus of point F on the $\omega$-$\omega_F$ plane using two-parameter continuation as shown in Figure 6. This diagram helps us determine the minimum safe operating frequency. By staying to the right side of this boundary, it is guaranteed that the blue branch of the stable solutions is the only attractor present. Two-parameter continuation is therefore a powerful technique that can be used to aid paramter tuning whilst designing an extremum seeking controller.

Lastly, we further investigate the nature of the instabilities in the blue branch using the magnified view in panel b. Two resonance peaks are observed. They correspond to the two natural frequencies of the open-loop aircraft as shown in Figure 7 (obtained using continuation by forcing the elevator at 0.5 deg amplitude). In this example, the short period mode becomes unstable due to the presence of the extremum seeking control and contributes to the formation of multiple stable solutions highlighted in panel C. It is known that the forcing frequency should be well-separated from the natural frequencies. However, we discovered using continuation that it is safe to operate around the phugoid frequency, i.e., only the short-period region should be avoided. This provides a powerful capability for controller design and paramter tuning, especially in highly nonlinear systems.

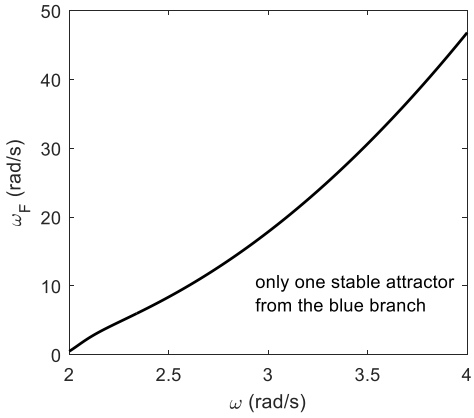


Figure 6. Two-parameter continuation of point F.

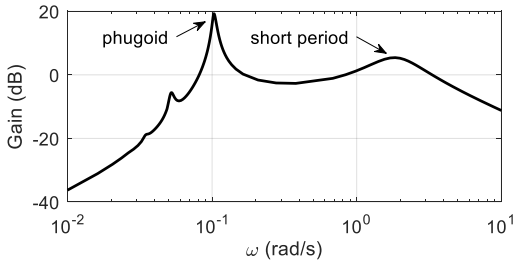


Figure 7. Open-loop nonlinear frequency response.

Results in this section have exemplified the potentially complex dynamics in a harmonically-forced system in general, and in an extremum-seeking controller in particular. Continuation not only provides a method to systematically characterise these behaviours, but can also be used to aid controller tuning via running a series of parameter sweeps. This argument has been made in previous studies on equilibrium bifurcation analysis (no harmonic forcing) [25], but it is even more important here because time simulations like those shown in Figure 4 are more computationally expensive to run due to the wide frequency separation between the forcing term and the plant's dynamics.

## V. Conclusion

The use of harmonically-forced bifurcation analysis to analyse a nonlinear extremum seeking controller has been presented. Our results have demonstrated that this approach provides a powerful framework for analysing complex nonlinear extremum seeking systems where existing approximations can be mathematically impractical or restrictive. Further developments in the topic should explore a realistic example, which exemplifies both the capability of continuation as well as the advantages of the extremum seeking method.

## Acknowledgment

We are grateful to NASA Langley Research Center, specifically Kevin Cunningham and Gautam Shah, for providing the GTT model.

## References

1. Tan, Y., Moase, W.H., Manzie, C., Nešić, D., Mareels, I.M.Y.: Extremum seeking from 1922 to 2010. In: Proceedings of the 29th Chinese Control Conference, 29-31 July 2010 2010, pp. 14-26
2. Krstić, M., Wang, H.-H.: Stability of extremum seeking feedback for general nonlinear dynamic systems. Automatica **36**(4), 595-601 (2000). doi:10.1016/S0005-1098(99)00183-1
3. Hsin-Hsiung, W., Yeung, S., Krstić, M.: Experimental application of extremum seeking on an axial-flow compressor. IEEE Transactions on Control Systems Technology **8**(2), 300-309 (2000). doi:10.1109/87.826801
4. Chen, J.-H., Yau, H.-T., Hung, W.: Design and Study on Sliding Mode Extremum Seeking Control of the Chaos Embedded Particle Swarm Optimization for Maximum Power Point Tracking in Wind Power Systems. Energies **7**(3), 1706-1720 (2014). doi:10.3390/en7031706
5. Binetti, P., Ariyur, K.B., Krstić, M., Bernelli, F.: Formation Flight Optimization Using Extremum Seeking Feedback. Journal of Guidance, Control, and Dynamics **26**(1), 132-142 (2003). doi:10.2514/2.5024
6. Killingsworth, N., Krstić, M.: Auto-tuning of PID controllers via extremum seeking. In: Proceedings of the 2005, American Control Conference, 2005., 8-10 June 2005 2005, pp. 2251-2256 vol. 2254
7. Hsin-Hsiung, W., Krstić, M.: Extremum seeking for limit cycle minimization. IEEE Transactions on Automatic Control **45**(12), 2432-2436 (2000). doi:10.1109/9.895589
8. Nešić, D.: Extremum Seeking Control: Convergence Analysis. European Journal of Control **15**(3), 331-347 (2009). doi:10.3166/ejc.15.331-347
9. Haring, M., van de Wouw, N., Nešić, D.: Extremum-seeking control for nonlinear systems with periodic steady-state outputs. Automatica **49**(6), 1883-1891 (2013). doi:doi.org/10.1016/j.automatica.2013.02.061
10. MathWorks: Simulink Control Design Release Notes. https://uk.mathworks.com/help/slcontrol/release-notes.html (2021). Accessed 21 February 2022
11. Dewasme, L., Vande Wouwer, A.: Model-Free Extremum Seeking Control of Bioprocesses: A Review with a Worked Example. Processes **8**(10) (2020). doi:10.3390/pr8101209
12. Ariyur, K.B., Krstić, M.: Real-Time Optimization by Extremum-Seeking Control, 1 ed. Real-Time Optimization by Extremum-Seeking Control. John Wiley & Sons, (2003)
13. Zhang, C., Ordonez, R.: Extremum-Seeking Control and Applications A Numerical Optimization-Based Approach, 1 ed. Advances in Industrial Control. Springer, London (2012)
14. Trollberg, O., Carlsson, B., Jacobsen, E.W.: Extremum seeking control of the CANON process—Existence of multiple stationary solutions. Journal of Process Control **24**(2), 348-356 (2014). doi:10.1016/j.jprocont.2013.11.007
15. Trollberg, O., Jacobsen, E.W.: On Bifurcations of the Zero Dynamics - Connecting Steady-State Optimality to Process Dynamics. In: IFAC-PapersOnLine, 2015/01/01/ 2015, vol. 8, pp. 170-175
16. Trollberg, O., Jacobsen, E.W.: Non-Uniqueness of Stationary Solutions in Extremum Seeking Control. In: arXiv preprint arXiv:1802.08520. (2018)
17. Trollberg, O.: On Real-Time Optimization using Extremum Seeking Control and Economic Model Predictive Control with Applications to Bioreactors and Paper Machines. KTH Royal Institute of Technology (2017)
18. Nguyen, D.H., Lowenberg, M.H., Neild, S.A.: Frequency-Domain Bifurcation Analysis of a Nonlinear Flight Dynamics Model. Journal of Guidance, Control, and Dynamics **44**(1), 138-150 (2021). doi:10.2514/1.G005197
19. Nguyen, D.H., Lowenberg, M.H., Neild, S.A.: Effect of Actuator Saturation on Pilot-Induced Oscillation: a Nonlinear Bifurcation Analysis. Journal of Guidance, Control, and Dynamics **44**(5), 1018-1026 (2021). doi:10.2514/1.G005840
20. Didenko, Y., Dolotovsky, A., Gorelov, S., Ivakha, V., Motovilov, V., Tarasov, A., Chochiev, V.: The specific features of FBW control laws of advanced regional jet. In: IFAC Proceedings Volumes, 2007/01/01/ 2007, vol. 7, pp. 129-134
21. Holzapfel, F., Heller, M., Weingartner, M., Sachs, G., da Costa, O.: Development of control laws for the simulation of a new transport aircraft. Proceedings of the Institution of Mechanical Engineers, Part G: Journal of Aerospace Engineering **223**(2), 141-156 (2009). doi:10.1243/09544100jaero309
22. Niedermeier, D., Lambregts, A.A.: Fly-by-wire augmented manual control - Basic design considerations. In: 28th International Congress of the Aeronautical Sciences, Brisbane, Australia, 23-28 September 2012. ICAS
23. Mehra, R., Carroll, J.: Bifurcation analysis of aircraft high angle-of-attack flight dynamics. Paper presented at the 6th Atmospheric Flight Mechanics Conference, Danvers, MA, 11-13 August 1980
24. Carroll, J.V., Mehra, R.K.: Bifurcation Analysis of Nonlinear Aircraft Dynamics. Journal of Guidance, Control, and Dynamics **5**(5), 529-536 (1982). doi:10.2514/3.56198
25. Sharma, S., Coetzee, E.B., Lowenberg, M.H., Neild, S.A., Krauskopf, B.: Numerical continuation and bifurcation analysis in aircraft design: an industrial perspective. Philosophical Transactions of the Royal Society A: Mathematical, Physical and Engineering Sciences **373**(2051), 20140406 (2015). doi:doi:10.1098/rsta.2014.0406
26. Jahnke, C.C., Culick, F.E.C.: Application of bifurcation theory to the high-angle-of-attack dynamics of the F-14. Journal of Aircraft **31**(1), 26-34 (1994). doi:10.2514/3.46451
27. Gill, S.J., Lowenberg, M.H., Neild, S.A., Crespo, L.G., Krauskopf, B., Puyou, G.: Nonlinear Dynamics of Aircraft Controller Characteristics Outside the Standard Flight Envelope. Journal of Guidance, Control, and Dynamics **38**(12), 2301-2308 (2015). doi:10.2514/1.G000966
28. Gill, S.J., Lowenberg, M.H., Neild, S.A., Crespo, L.G., Krauskopf, B.: Impact of Controller Delays on the Nonlinear Dynamics of Remotely Piloted Aircraft. Journal of Guidance, Control, and Dynamics **39**(2), 292-300 (2016). doi:10.2514/1.G001222
29. Coetzee, E., Krauskopf, B., Lowenberg, M.H.: The Dynamical Systems Toolbox: Integrating AUTO into Matlab. Paper presented at the 16th US National Congress of Theoretical and Applied Mechanics, State College, PA, 27 June-2 July 2010
30. Doedel, E.J.: AUTO-07P, Continuation and Bifurcation Software for Ordinary Differential Equations, Ver. 07P. http://www.macs.hw.ac.uk/~gabriel/auto07/auto.html (2007). Accessed 21 February 2022